Dodecamethyl-*closo*-dodecaborate(2−)

Toralf Peymann, Carolyn B. Knobler, Saeed I. Khan, and M. Frederick Hawthorne*

Department of Chemistry and Biochemistry, University of California, Los Angeles,
405 Hilgard Avenue, Los Angeles, California 90095-1569

Bis(tetraethylammonium) dodecamethyl-*closo*-dodecaborate(2−), [NEt$_4$]$_2$[*closo*-B$_{12}$Me$_{12}$], [NEt$_4$]$_2$**2**, was prepared employing modified Friedel−Crafts reaction conditions from [NEt$_4$]$_2$[*closo*-B$_{12}$H$_{12}$], [NEt$_4$]$_2$**1**, trimethylaluminum, and methyl iodide. The [NEt$_4$]$_2$**2** salt provides sufficient solubility in water to allow the synthesis of the important alkali metal salts A$_2$**2** (A = Li, Na, K, Rb, Cs) using cation-exchange procedures. The solid state structure of colorless [AsPh$_4$]$_2$**2** reveals a nearly perfect icosahedral B$_{12}$ cluster with B−B bonds ranging from 1.785(3) to 1.807(3) Å and B−C bonds of 1.597(3)−1.625(3) Å. In contrast, the crystal structure of dark-red [Py$_2$CH$_2$]**2** (obtained from [NEt$_4$]$_2$**2** and [Py$_2$CH$_2$]Br$_2$) contains a distorted icosahedral dianion [B−B = 1.740(13)−1.811-(14) Å, B−C = 1.591(13)−1.704(13) Å]. In the [Py$_2$CH$_2$]**2** salt, the dianion **2**$^{2−}$ and its dipositive dipyridini-omethane counterion form a red charge-transfer complex. One-electron oxidation of **2**$^{2−}$ by ceric(IV) ammonium nitrate affords the blue, air-stable radical [*hypercloso*-B$_{12}$Me$_{12}$]$^{•−}$, dodecamethyl-*hypercloso*-dodecaborate(1−), **2**$^{•−}$, isolated as the PPN salt. X-ray crystallography reveals that the geometries of the B$_{12}$ clusters observed in *hypercloso*-[PPN]**2** and *closo*-[AsPh$_4$]$_2$**2** are identical and essentially undistorted icosahedra. The anion in the [PPN]**2** structure contains B−B bonds ranging from 1.784(8) to 1.806(7) Å and a range of B−C bonds from 1.596(7) to 1.616(7) Å.

The icosahedral (car)boranes [*closo*-C$_n$B$_{12−n}$H$_{12}$]$^{n−2}$ (n = 0−2) are paradigms of nonmetallic inorganic clusters, although the presence of their acidic C−H vertexes for n = 1,2 has spawned abundant offspring in the form of C-substituted, organic carborane derivatives.[1] In recent years, several methods for the B-alkylation of icosahedral carboranes have been reported as well.[2] The preparation of the permethylated carboranes [*closo*-C$_n$B$_{12−n}$Me$_{12}$]$^{n−2}$ (n = 1, 2)$^{3−5}$ resulted in species comprising an approximately spherical carborane framework and a lipophilic hydrocarbon surface. This confluence of polyhedral carborane and hydrocarbon chemistry promises to combine the unique physical properties of the boranes, such as their extreme kinetic stabilities and three-dimensional aromaticity, with the synthetic arsenal of organic methodology. First examples of this fruitful marriage, such as the Barton reaction[6] of nitrosyl chloride and deca-*B*-methyl-1-hydroxymethyl-1,12-dicarba-*closo*-dodecabo-rane(12) and the halogenated derivatives *closo*-(CH)$_2$B$_{10}$-(CHCl$_2$)$_{10}$[7] and [*closo*-CB$_{11}$(CF$_3$)$_{12}$]$^−$,[8] have emerged. Potential applications for these hybrid materials exist in the areas of nanoscale architectures,[9] dendrimer chemistry,[10] drug delivery,[11] and weakly coordinating anions.[12]

Relative to the isoelectronic carboranes, progress in the synthetic chemistry of [*closo*-B$_{12}$H$_{12}$]$^{2−}$, **1**$^{2−}$,[13] has been impeded by its higher symmetry (point group I_h), which results in a larger number of polysubstituted isomers, and by the absence of the easily functionalized carborane C−H vertexes. To avoid the problem of isomers, sustain the aesthetically pleasing symmetry of the borane cluster, and employ the anionic icosahedral scaffold for larger architectures, research has recently focused on the perfunctionalization of the B$_{12}$ cluster exemplified by the camouflaged anions [*closo*-B$_{12}$(OH)$_{12}$]$^{2−}$[14] and [*closo*-B$_{12}$-(BSe$_3$)$_6$]$^{8−}$.[15] In two previous communications, we described the initial preparation of diamagnetic [*closo*-B$_{12}$Me$_{12}$]$^{2−}$, **2**$^{2−}$,[16] followed by its one-electron oxidation product, paramagnetic [B$_{12}$Me$_{12}$]$^{•−}$, **2**$^{•−}$.[17] The purpose of this report is to disclose full details of the synthesis and characterization of **2**$^{2−}$ as well as the preparation of useful salts of **2**$^{2−}$.

Results and Discussion

The synthesis of the tetra-*n*-butylammonium salt of **2**$^{2−}$, [N(*n*-Bu)$_4$]$_2$**2**, which requires 11 days for complete permethylation of **1**$^{2−}$, was reported previously.[16] In this article, the preparation of the tetraethylammonium salt of **2**$^{2−}$, [NEt$_4$]$_2$**2**, is described.

(1) Grimes, R. N. *Carboranes*; Academic Press: New York, 1970.
(2) Jiang, W.; Knobler, C. B.; Curtis, C. E.; Mortimer, M. D.; Hawthorne, M. F. *Inorg. Chem.* **1995**, *34*, 3491 and references therein.
(3) King, B. T.; Janousek, Z.; Grüner, B.; Trammell, M.; Noll, B. C.; Michl, J. *J. Am. Chem. Soc.* **1996**, *118*, 3313.
(4) Jiang, W.; Knobler, C. B.; Mortimer, M. D.; Hawthorne, M. F. *Angew. Chem., Int. Ed. Engl.* **1995**, *34*, 1332.
(5) Tsang, C. W.; Xie, Z. *Chem. Commun.* **2000**, 1839.
(6) Jiang, W.; Knobler, C. B.; Mortimer, M. D.; Hawthorne, M. F. *Angew. Chem., Int. Ed. Engl.* **1996**, *35*, 2536.
(7) Herzog, A.; Knobler, C. B.; Hawthorne, M. F. *Angew. Chem., Int. Ed.* **1998**, *37*, 1552.
(8) King, B. T.; Michl, J. *J. Am. Chem. Soc.* **2000**, *122*, 10255.

(9) Nalwa, H. S. *Handbook of Nanostructured Materials and Nanotech-nology*; Academic Press: San Diego, 1999.
(10) Newkome, G. R., Moorefield, C. N., Vögtle, F. *Dendritic Molecules*; VCH: New York, 1996.
(11) Rolland, A. *Pharmaceutical Particle Carriers: Therapeutic Applica-tions*; Marcel Dekker: New York, 1993.
(12) Reed, C. A. *Acc. Chem. Res.* **1998**, *31*, 133.
(13) (a) Pitochelli, A. R.; Hawthorne, M. F. *J. Am. Chem. Soc.* **1960**, *82*, 3228. (b) Miller, H. C.; Miller, N. E.; Muetterties, E. L. *Inorg. Chem.* **1964**, *3*, 1456. (c) Muetterties, E. L.; Knoth, W. H. *Polyhedral Boranes*; M. Dekker: New York, 1968; pp 104−168.
(14) Peymann, T.; Herzog, A.; Knobler, C. B.; Hawthorne, M. F. *Angew. Chem., Int. Ed.* **1999**, *38*, 1062.
(15) Küper, J.; Conrad, O.; Krebs, B. *Angew. Chem., Int. Ed. Engl.* **1997**, *36*, 1903.
(16) Peymann, T.; Knobler, C. B.; Hawthorne, M. F. *J. Am. Chem. Soc.* **1999**, *121*, 5601.
(17) Peymann, T.; Knobler, C. B.; Hawthorne, M. F. *Chem. Commun.* **1999**, 2039.

Table 1. Crystallographic Data for [AsPh$_4$]$_2$**2**, [Py$_2$CH$_2$]**2**,[16] and [PPN]**2**[17]

	[AsPh$_4$]$_2$**2**	[Py$_2$CH$_2$]**2**·CH$_3$CN	[PPN]**2**
formula	C$_{60}$H$_{76}$As$_2$B$_{12}$	C$_{25}$H$_{51}$B$_{12}$N$_3$	C$_{48}$H$_{66}$B$_{12}$NP$_2$
fw	1076.77	523.42	878.04
temp (K)	100(2)	298(2)	298(2)
cryst syst	monoclinic	orthorhombic	monoclinic
space group	$P2_1/c$	$Pc2_1n$	$C2/c$
a (Å)	12.771(3)	9.715(7)	34.56(3)
b (Å)	12.242(3)	15.05(1)	9.342(8)
c (Å)	19.454(5)	22.82(2)	18.69(2)
β (deg)	108.215(5)		122.22(2)
V (Å^3)	2889(1)	3337(4)	5120(7)
Z	2	4	4
d (g cm^{-3})	1.238	1.04	1.1
μ (cm^{-1})	1.195	3.7	1.2
R^a	0.031	0.074	0.066
$R_w{}^b$	0.077	0.184	0.167

^{a} $R = \sum||F_o| - |F_c||/|F_o|$. ^{b} $R_w = [\sum w(|F_o| - |F_c|)^2/\sum w(|F_o|^2]^{1/2}$.

The permethylation of the dianion in [NEt$_4$]$_2$**1** to obtain [NEt$_4$]$_2$**2** requires 3 weeks due to the poor solubility of the starting material in the trimethylaluminum solvent. Nevertheless, the route employing [NEt$_4$]$_2$**1** is advantageous because the product, [NEt$_4$]$_2$**2**, is more hydrophilic relative to [N(*n*-Bu)$_4$]$_2$**2**. This solubility feature allows the cation-exchange of the NEt$_4{}^+$ cation to afford the alkali metal salts A$_2$**2** (A = Li, Na, K, Rb, Cs). These salts cannot be obtained via ion exchange of the previously described lipophilic [N(*n*-Bu)$_4$]$_2$**2** salt because the latter is rather insoluble in aqueous solvent systems. The more water soluble A$_2$**2** salts such as Na$_2$**2** are important for the study of the liposomal delivery of the amphiphilic anion **2**$^{2-}$ in the context of boron neutron capture therapy (BNCT) of cancer.[18] Furthermore, the Na$_2$**2** salt functions as the starting material for the synthesis of paramagnetic Na**2** (vide infra). Both sodium salts, Na$_2$**2** and Na**2**, and their excited states are currently being studied by vibrational and luminescence spectroscopy,[19] investigations that demand a Raman- and infrared-silent counterion such as sodium.

Colorless crystals of [AsPh$_4$]$_2$**2**, prepared by metathesis of [NEt$_4$]$_2$**2** and [AsPh$_4$]Cl in methanol, were obtained from acetone/toluene and subjected to single-crystal X-ray diffraction analysis. The salt crystallized in the monoclinic space group $P2_1/c$ (Table 1). Most importantly, the centrosymmetric anion **2**$^{2-}$ (Figure 1) displayed nearly ideal icosahedral symmetry as indicated by the narrow range of B–B and B–C distances of [AsPh$_4$]$_2$**2** (Table 2). Broader ranges of B–B and B–C bond lengths are observed for the anion of the [Py$_2$CH$_2$]**2** salt,[16] and this distortion may be attributed to the charge-transfer interaction between cation and anion (Figure 2). In the structures of [AsPh$_4$]$_2$**2** and [PPN]**2**[17] (vide infra), the anions have crystallographic symmetry (both are centrosymmetric), whereas in [Py$_2$CH$_2$]**2** the anion has no symmetry. Unfortunately, the estimated standard deviations are much higher for the latter structure; nevertheless, the structural distortion of the anion of [Py$_2$CH$_2$]**2** can be seen by the extension of one extreme of the bond length ranges. For example, the longest B–B distance is nearly identical in all three structures (Table 2). However, in the structure of [Py$_2$CH$_2$]**2** there are 17 B–B bond lengths (slightly over half of the total of 30 B–B bonds) ranging from 1.740 to 1.783 Å, i.e., less than the shortest B–B distance found in the other two anions. Likewise, the shortest B–C distance in all three structures is essentially the same. But there are eight

(18) Feakes, D. A.; Shelly, K.; Knobler, C. B.; Hawthorne, M. F. *Proc. Natl. Acad. Sci. U.S.A.* **1994**, *92*, 3029.
(19) Zink, J. I.; Hawthorne, M. F. Unpublished results.
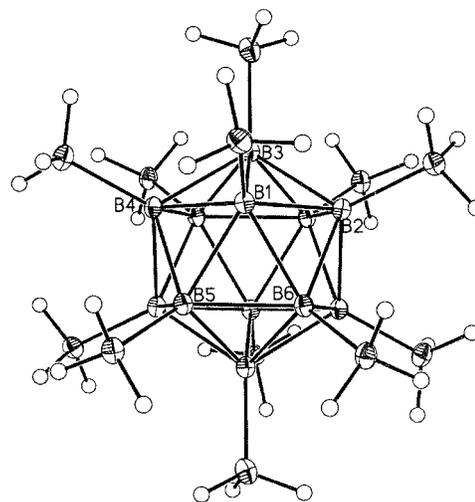
Figure 1. ORTEP diagram of the **2**$^{2-}$ anion of [AsPh$_4$]$_2$**2**, with ellipsoids drawn at 30% probability.
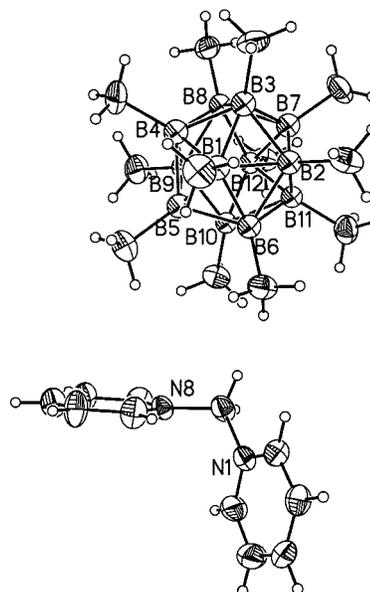
Figure 2. Charge-transfer interaction of [Py$_2$CH$_2$]$^{2+}$ and **2**$^{2-}$. Thermal ellipsoids are drawn at 30% probability.

Table 2. Relevant Bond Distances [Å] of Salts of **2**$^{2-}$ and **2**$^{•-}$

	[AsPh$_4$]$_2$**2**	[Py$_2$CH$_2$]**2**·CH$_3$CN	[PPN]**2**
B–B	1.785(3)–1.807(3)	1.740(13)–1.811(14)	1.784(8)–1.806(7)
B–C	1.597(3)–1.625(3)	1.591(13)–1.704(13)	1.596(9)–1.616(7)

B–C distances in [Py$_2$CH$_2$]**2** in the range 1.639–1.704 Å, longer than any B–C distance found in the other two anions.

Whereas the electrochemical oxidation of **1**$^{2-}$ was reported to yield the dimeric species [*closo*-B$_{24}$H$_{23}$]$^{3-}$,[20] the one-electron oxidation of **2**$^{2-}$ by ceric ion afforded the radical monoanion **2**$^{•-}$ (Scheme 1).[17] A comparison of the bond distances of both permethylated anions, diamagnetic **2**$^{2-}$ and paramagnetic **2**$^{•-}$, finds the two icosahedra to be of identical geometry within experimental error. Surprisingly, the loss of one electron from a HOMO of **2**$^{2-}$ does not affect the geometry of the resulting **2**$^{•-}$ relative to **2**$^{2-}$. This result differs from the observation in the [B$_{12}$(OCH$_2$Ph)$_{12}$]$^{n-}$ ($n = 0-2$) series, in which a loss of cluster electron density results in the lengthening of discrete

(20) Wiersema, R. J.; Middaugh, R. L. *J. Am. Chem. Soc.* **1967**, *89*, 5079.

Scheme 1. Synthesis of **2**$^{2-}$ and Its Oxidation to **2**$^{•-}$ Compared to the Oxidation of **1**$^{2-}$
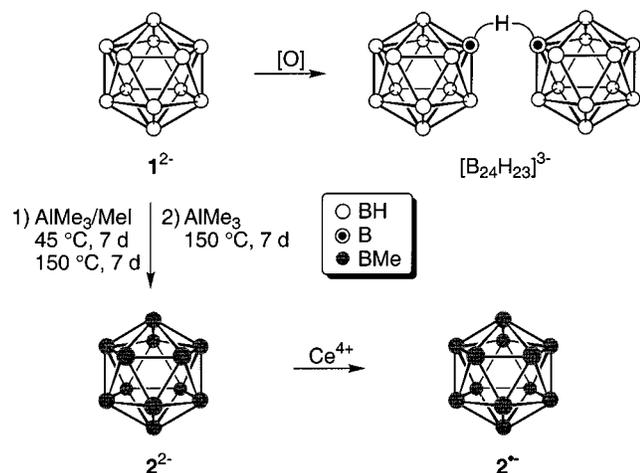
B−B bonds and a shortening of B−O bonds due to back-bonding.[21]

The UV−visible spectrum of Na$_2$**2** in acetonitrile solution displays a major absorption band at 242 nm ($\epsilon = 4.7 \times 10^3$). In the UV−visible spectrum of [Py$_2$CH$_2$]**2**, this band is shifted to 258 nm ($\epsilon = 1.1 \times 10^4$) and two shoulders of this band are observed at 318 nm ($\epsilon = 175$) and 442 nm ($\epsilon = 57$). These spectroscopic differences are attributed to the charge-transfer interaction between the cation and **2**$^{2-}$.

Both Raman and infrared spectra of the highly symmetric **2**$^{2-}$ anion, as its sodium salt, exhibit few absorption bands. In the infrared spectrum of Na$_2$**2** the most intense bands appear between 2935 and 2860 cm^{-1} and are assigned to the vibrations of the methyl groups. Another intense absorption band at 1290 cm^{-1} is attributed to a B−B vibrational breathing mode.[22] In the fingerprint region, two bands of medium intensity at 1125 (ν_{B-C}) and 894 (ν_{B-B} breathing mode) cm^{-1} are observed. The frequencies of the icosahedral B−B breathing modes are shifted to higher energies relative to the two major bands of Na$_2$**1** at 1070 and 720 cm^{-1}.[23] In the Raman spectrum of Na$_2$**2** the vibrations of the methyl groups are observed between 2922 and 2829 cm^{-1}. The most intense absorption band at 453 cm^{-1} is due to the B−B vibration.

In conclusion, the permethylated [*closo*-B$_{12}$Me$_{12}$]$^{2-}$ anion, **2**$^{2-}$, has been described. This highly symmetric species comprises a periphery of 12 methyl groups and a dianionic core. Similar to the isolobal, permethylated carboranes, the methyl sheath of **2**$^{2-}$ may potentially be derivatized. In contrast to the parent anion [*closo*-B$_{12}$H$_{12}$]$^{2-}$ that dimerizes upon electrochemical oxidation, the dianionic core of **2**$^{2-}$ is readily oxidized by ceric ion to the paramagnetic species [*hypercloso*-B$_{12}$Me$_{12}$]$^{•-}$, **2**$^{•-}$, ($E_{1/2} = 0.44$ V).[17] The crystal structures of two different salts of the [*closo*-B$_{12}$Me$_{12}$]$^{2-}$ anion, [Py$_2$CH$_2$]**2** and [AsPh$_4$]$_2$**2**, and of paramagnetic [PPN]**2** have been determined by X-ray crystallography. In the red [Py$_2$CH$_2$]**2** salt, the B$_{12}$ icosahedron is distorted due to a charge-transfer interaction, whereas in both [AsPh$_4$]$_2$**2** and [PPN]**2** the icosahedral symmetry of the B$_{12}$ cluster is conserved. Furthermore, the icosahedral **2**$^{2-}$ anion has been characterized by vibrational and UV−visible spectroscopy. Besides the B−C and C−H vibrations, both IR and Raman

(21) Peymann, T.; Knobler, C. B.; Hawthorne, M. F. *Angew. Chem., Int. Ed.*, submitted.
(22) Leites, L. A. *Chem. Rev.* **1992**, *92*, 279.
(23) Muetterties, E. L.; Merrifield, R. E.; Miller, H. C.; Knoth, W. H., Jr.; Downing, J. R. *J. Am. Chem. Soc.* **1962**, *84*, 2506.

spectra consist of only a few breathing modes of the B$_{12}$ icosahedral framework due to the high symmetry of the anion.

Experimental Section

CAUTION! Trimethylaluminum is moisture sensitive and pyrophoric, and should be handled with extreme caution. Since the procedure below employs AlMe$_3$ in large excess, mixtures should be handled with care throughout the procedure, until the neutralization and disposal of excess AlMe$_3$ is assured. Particular care should be employed during the extraction of excess AlMe$_3$ with pentane because of the low flash point of this solvent.

General Procedures. All manipulations involving trimethylaluminum (97%, used as received from Aldrich) were conducted under an atmosphere of nitrogen. Pentane was dried and distilled over CaH$_2$ prior to use. All other solvents were reagent grade. Cs$_2$[*closo*-B$_{12}$H$_{12}$][13] was obtained as a gift from DuPont and ion-exchanged to produce the tetraethylammonium salt.

Proton NMR spectra were recorded with a Bruker ARX-400 spectrometer. The ^{11}B NMR spectra were obtained with a Bruker AM-500 spectrometer at 160 MHz and were externally referenced to BF$_3$·Et$_2$O; peaks upfield of the reference are designated as negative. Infrared spectra were measured on KBr pellets with a Nicolet-Nexus 470 spectrometer. Raman spectra were obtained on solid samples in sealed evacuated capillaries using a Spex 1401 double monochromator equipped with an RCA C31034 photomultiplier tube; excitation was provided by a Coherent I-90 Argon laser (514.5 nm, typical power 100 mW), and data were collected with a Stanford Research System SR400 photon counter. Electrospray ionization mass spectra (ESI-MS) were recorded by injecting an aqueous sample solution into an ionspray source with the mass spectrometer operating in the negative-ion mode.

Bis(tetraethylammonium) Dodecamethyl-*closo*-dodecaborate-(2−), [NEt$_4$]$_2$2. Methyl iodide (2.30 mL, 38 mmol) was added via a syringe to a suspension of [NEt$_4$]**1** (0.63 g, 1.60 mmol) in trimethylaluminum (10 mL) under dry nitrogen. The mixture was kept for 1 week at 45 °C followed by heating with a heating mantle at 150 °C for 1 week. After cooling to room temperature, the volatiles were removed in vacuo, and the oily product mixture was stirred under nitrogen in dry pentane (100 mL) to extract residual trimethylaluminum. The pentane was decanted under nitrogen, and ethanol (50 mL) was added cautiously to the residue. After stirring for 1 h, the solid was separated by filtration, washed with water, and dissolved in acetonitrile (50 mL). Following filtration, acetonitrile was removed in vacuo and the obtained solid, which consists mainly of iodoundecamethyl-*closo*-dodecaborate-(2−), was heated at the reflux temperature for 1 week with trimethylaluminum (10 mL) and worked up as described above. After recrystallization from ethanol/acetonitrile, colorless [NEt$_4$]$_2$**2** (0.72 g, 1.30 mmol, 79%) was obtained.

^{1}H NMR (400 MHz, acetone-d_6): 3.47 (q, N−CH$_2$, 16 H), 1.37 (m, C−Me, 24 H), −0.51 ppm (s, B−Me, 36 H). ^{11}B NMR (160 MHz, DMSO): −10.8 ppm (s, B−Me).

Bis(tetraphenylarsonium) Dodecamethyl-*closo*-dodecaborate-(2−), [AsPh$_4$]$_2$2. A sample of [NEt$_4$]$_2$**2** (80 mg, 0.14 mmol) was dissolved in methanol/acetonitrile, and a methanol solution of [AsPh$_4$]-Cl (240 mg, 0.56 mmol) was added. Immediately, a colorless solid precipitated, which was separated by filtration and washed with methanol. After drying, colorless [AsPh$_4$]$_2$**2** (140 mg, 0.13 mmol, 93%) was obtained.

(Dipyridinio)methane Dodecamethyl-*closo*-dodecaborate(2−), [Py$_2$CH$_2$]2. A sample of [NEt$_4$]$_2$**2** (80 mg, 0.14 mmol) was dissolved in water/acetonitrile, and a solution of [Py$_2$CH$_2$]Br$_2$ (120 mg, 0.35 mmol) in water/acetonitrile was added. A dark-orange oil formed, which solidified overnight. The solid was separated by filtration and recrystallized from acetonitrile/ethanol to give red crystals of [Py$_2$CH$_2$]**2**. UV/vis (MeCN): λ (ϵ) = 258 (1.1 × 10^4), 318 (175), 442 nm (57).

Synthesis of A$_2$2 (A = Alkali Metal Cation). A sample of [NEt$_4$]$_2$**2** was dissolved in 40% acetonitrile and subjected to an ion exchange on a strong cation-exchange resin column (BIO-RAD AG 50W-X2 200−400 mesh). The volatiles were removed from the eluate in vacuo, and the residue was dried on a lyophilizer to yield the respective alkali metal salt, A$_2$**2**. No tetraethylammonium resonance was observed by

^{1}H NMR spectroscopy. Na$_2$**2**: UV/vis (MeCN): λ (ϵ) = 242 (4.7 $\times$ 10^3). IR (KBr) ν [cm^{-1}]: 2935 (m, C$-$H), 2908 (m, C$-$H), 2881 (m, C$-$H), 2860 (s, C$-$H), 1637 (w), 1617 (w), 1441 (w), 1290 (s, B$-$C), 1125 (m, B$-$B), 894 (m, B$-$B). Raman ν [cm^{-1}]: 2922 (m, C$-$H), 2907 (m, C$-$H), 2896 (m, C$-$H), 2829 (s, C$-$H), 453 (s, B$-$B), 431 (m, B$-$B), 422 (s, B$-$C), 412 (m, B$-$C), 211 (w).

Crystal Structure Determination of [AsPh$_4$]$_2$2. A colorless crystal of [AsPh$_4$]$_2$**2**, obtained from acetone/toluene, was placed on a fiber and mounted on a Bruker diffractometer. Unit cell parameters were determined from a least-squares fit of 991 accurately centered reflections (4.7° < 2θ < 55.4°). Data were collected at 100 K in the $\theta-2\theta$ scan mode. Of the 6918 unique reflections measured, 5094 were considered observed [$I > 2\sigma(I)$] and were used in the subsequent structure analysis. Data were corrected for Lorentz and polarization effects and for secondary extinction and absorption. Programs used in this work include those provided in the Bruker SMART package.

Atoms were located by use of heavy atom methods. All non-hydrogen atoms were refined with anisotropic parameters. All hydrogen atoms have been refined. All phenyl groups were included as rigid C$_6$ hexagons, C$-$C = 139.5 pm, angles 120°. Hydrogen atoms were assigned isotropic displacement values based approximately on the value of the attached atom.

Supporting Information Available: IR and Raman spectra of Na$_2$**2** and X-ray crystallographic files in CIF format for the structure determinations of [AsPh$_4$]$_2$**2**, [Py$_2$CH$_2$]**2**, and [PPN]**2**. This material is available free of charge via the Internet at http://pubs.acs.org.

IC0010398